

MIT Open Access Articles

*A Transition in Brain State during
Propofol-Induced Unconsciousness*

The MIT Faculty has made this article openly available. **Please share** how this access benefits you. Your story matters.

Citation: Mukamel, E. A., E. Pirondini, B. Babadi, K. F. K. Wong, E. T. Pierce, P. G. Harrell, J. L. Walsh, et al. "A Transition in Brain State During Propofol-Induced Unconsciousness." *Journal of Neuroscience* 34, no. 3 (January 15, 2014): 839–845.

As Published: <http://dx.doi.org/10.1523/jneurosci.5813-12.2014>

Publisher: Society for Neuroscience

Persistent URL: <http://hdl.handle.net/1721.1/91534>

Version: Final published version: final published article, as it appeared in a journal, conference proceedings, or other formally published context

Terms of Use: Article is made available in accordance with the publisher's policy and may be subject to US copyright law. Please refer to the publisher's site for terms of use.



A Transition in Brain State during Propofol-Induced Unconsciousness

Eran A. Mukamel,^{1,2} Elvira Pirondini,³ Behtash Babadi,³ Kin Foon Kevin Wong,³ Eric T. Pierce,³ P. Grace Harrell,³ John L. Walsh,³ Andres F. Salazar-Gomez,³ Sydney S. Cash,⁴ Emad N. Eskandar,⁵ Veronica S. Weiner,⁶ Emery N. Brown,^{3,7,8,9} and Patrick L. Purdon^{3,7}

¹Swartz Program for Theoretical Neuroscience, Harvard University, Cambridge, Massachusetts 02138, ²Center for Theoretical Biological Physics, University of California, San Diego, La Jolla, California 92093 and Computational Neurobiology Laboratory, Salk Institute for Biological Studies, San Diego, California 92037, ³Department of Anesthesia, Critical Care and Pain Medicine, Massachusetts General Hospital, Boston, Massachusetts 02114, ⁴Department of Neurology, Massachusetts General Hospital, Boston, Massachusetts 02114, ⁵Department of Neurosurgery, Massachusetts General Hospital, Boston, Massachusetts 02114, ⁶Department of Brain and Cognitive Science, Massachusetts Institute of Technology, Cambridge, Massachusetts 02139, ⁷Harvard Medical School, Boston, Massachusetts 02115, ⁸Division of Health Science and Technology, Harvard-Massachusetts Institute of Technology, Cambridge, Massachusetts 02139, and ⁹Institute for Medical Engineering and Sciences, Massachusetts Institute of Technology, Cambridge, Massachusetts 02139

Rhythmic oscillations shape cortical dynamics during active behavior, sleep, and general anesthesia. Cross-frequency phase-amplitude coupling is a prominent feature of cortical oscillations, but its role in organizing conscious and unconscious brain states is poorly understood. Using high-density EEG and intracranial electrocorticography during gradual induction of propofol general anesthesia in humans, we discovered a rapid drug-induced transition between distinct states with opposite phase-amplitude coupling and different cortical source distributions. One state occurs during unconsciousness and may be similar to sleep slow oscillations. A second state occurs at the loss or recovery of consciousness and resembles an enhanced slow cortical potential. These results provide objective electrophysiological landmarks of distinct unconscious brain states, and could be used to help improve EEG-based monitoring for general anesthesia.

Key words: α rhythm; anesthesia; cross-frequency coupling; propofol; Slow oscillation; unconsciousness

Introduction

Although the molecular actions of many anesthetic drugs at specific receptors are known (Brown et al., 2010), alterations in network dynamics that disrupt information processing and produce unconsciousness have remained elusive (Alkire et al., 2008). Loss of consciousness is accompanied by increased EEG power across a broad range of frequencies <40 Hz (Gugino et al., 2001; Feshchenko et al., 2004; Murphy et al., 2011; Purdon et al., 2013). Traditional analyses, including visual interpretation of EEG traces and time-frequency power spectral analysis, are computationally simple and play a central role in neurophysiology and clinical EEG applications. However, power spectral analysis treats the EEG as a collection of independent frequency bands, offering

limited insight into the modulation of network activity as a whole. Because cortical networks frequently express oscillations in multiple frequency bands simultaneously, nonlinear biophysical processes, such as neuronal spiking, induce cross-frequency coupling, which is undetectable by spectral analysis (Roopun et al., 2008). Identifying global brain states, such as sleep stages or general anesthesia-induced unconsciousness, remains a significant challenge for understanding cortical dynamics (Gervasoni et al., 2004). Moreover, an EEG-based framework for understanding brain state transitions during general anesthesia will be critical for improving patient monitoring to avoid complications, such as intraoperative awareness (Avidan et al., 2011).

We reasoned that critical information for identifying and characterizing distinct global brain states may be contained in patterns of coupling between distinct frequency bands. A simple form of cross-frequency interaction is phase-amplitude coupling, in which power within one frequency band waxes and wanes at specific phases of an underlying, lower-frequency rhythm (Jensen and Colgin, 2007). Phase-amplitude coupling is widespread during sleep, waking (He et al., 2010), and general anesthesia (Molaei-Ardekani et al., 2007; Breshears et al., 2010; Mukamel et al., 2011; Purdon et al., 2013) and has been related to attention and behavior in human and primate cortex (Canolty et al., 2006; Lakatos et al., 2008). In previous work, we discovered two forms of coupling between the phase of low-frequency activity (LFA, 0.1–2 Hz) and the amplitude of α rhythms (8–14 Hz) in

Received Dec. 19, 2012; revised Nov. 5, 2013; accepted Nov. 10, 2013.

Author contributions: E.A.M., E.N.B., and P.L.P. designed research; E.A.M., E.P., B.B., K.F.K.W., E.T.P., P.G.H., J.L.W., A.F.S.-G., S.S.C., E.N.E., V.S.W., E.N.B., and P.L.P. performed research; E.A.M., E.P., B.B., and K.F.K.W. analyzed data; E.A.M. and P.L.P. wrote the paper.

This work was supported by a Swartz Fellowship in Theoretical Neuroscience (E.A.M.), the University of California–San Diego Center for Biological Physics (E.A.M.), and National Institutes of Health Grants K99NS080911 (E.A.M.), DP2-OD006454 (P.L.P.), K25-NS057580 (P.L.P.), DP1-OD003646-01 (E.N.B.), R01-EB006385 (E.N.B., P.L.P.), and R01-MH071847 (E.N.B.).

The authors declare no competing financial interests.

Correspondence should be addressed to Dr. Patrick L. Purdon, Department of Anesthesia, Critical Care, and Pain Medicine, Building 149, Thirteenth Street, Room 4012, Charlestown, MA 02129-2060. E-mail: patrickp@nmr.mgh.harvard.edu.

DOI:10.1523/JNEUROSCI.5813-12.2014

Copyright © 2014 the authors 0270-6474/14/330839-07\$15.00/0

scalp EEG recordings during propofol general anesthesia (Mukamel et al., 2011; Purdon et al., 2013). One form of coupling occurred during the transitions to and from the unconscious state (“trough-max”), whereas the other occurred at deep levels of unconsciousness (“peak-max”) (Mukamel et al., 2011; Purdon et al., 2013). The cortical networks involved in these distinct modulation patterns, their frequency dependence, and their relationship to other brain states, such as burst suppression, are unclear. Here we investigate the cortical generators of these modulation patterns using source localization analysis and intracranial electrocorticography, analyze their frequency dependence, demonstrate these effects in individual subjects, and clarify their relationship to burst suppression. We find that these patterns of cross-frequency coupling reflect dynamics within distinct cortical networks and identify a transition in global brain state.

Materials and Methods

Subjects and recordings. Following approval from the Massachusetts General Hospital Human Research Committee, we induced and allowed recovery from general anesthesia in 10 healthy volunteers (5 male) using the intravenous anesthetic propofol (2,6 di-isopropyl-phenol). Propofol concentration increased in steps from 0 to 5 $\mu\text{g/ml}$ every 14 min, followed by gradual reduction (see Fig. 1*a*). We recorded 64 channel EEG using a BrainVision MRI Plus system (BrainAmp MRPlus, Brain-Products) with sampling rate 5 kHz, resolution 0.5 μV least significant bit, and bandwidth 0.016–1000 Hz. We also recorded galvanic skin response and plethysmography (PowerLab; AD Instruments). Electrodes, amplifiers, and filter settings provided accurate and unbiased recording of the entire frequency range analyzed in this study (0.1–50 Hz). A Bayesian method was used to estimate the time-varying probability of response (see Fig. 1*b*) (Smith et al., 2009). We defined the time of loss of consciousness (LOC), t_{LOC} , and return of consciousness (ROC), t_{ROC} , as the first and last times at which the median response probability was <0.05 .

EEG data were rereferenced using a Laplacian montage by subtracting the mean of each channel’s nearest neighbors (Nunez and Pilgreen, 1991). The Laplacian montage improves spatial localization of focal sources but attenuates EEG components with low spatial frequencies. Because these components tend to have low temporal frequencies, it is also found to attenuate low temporal frequencies. We verified that the reference choice had a minor impact on our measurement of phase-amplitude coupling by repeating the analysis using the average of mastoid electrodes as a reference. Raw signals, $x(t)$, were first smoothed using an anti-aliasing filter and downsampled to 250 Hz. We removed ultra-low-frequency drift by subtracting a piecewise quadratic spline fit to the signal with knots every 15 s. We rejected bad channels by visual inspection. We adopted a conservative procedure to remove low-frequency, large-amplitude EEG artifacts caused by movements while subjects were awake. We extracted the low-frequency signal, $x_{lo}(t)$, by applying a band-pass filter (0.2–6 Hz) and downsampling to 5 Hz, then applying a median filter (window size 30 s) to $|x_{lo}(t)|$. We defined artifacts as any time point for which $|x_{lo}(t)|$ was at least 10-fold greater than this local threshold. We excluded data within ± 5 s of any artifact on each channel. Power spectral

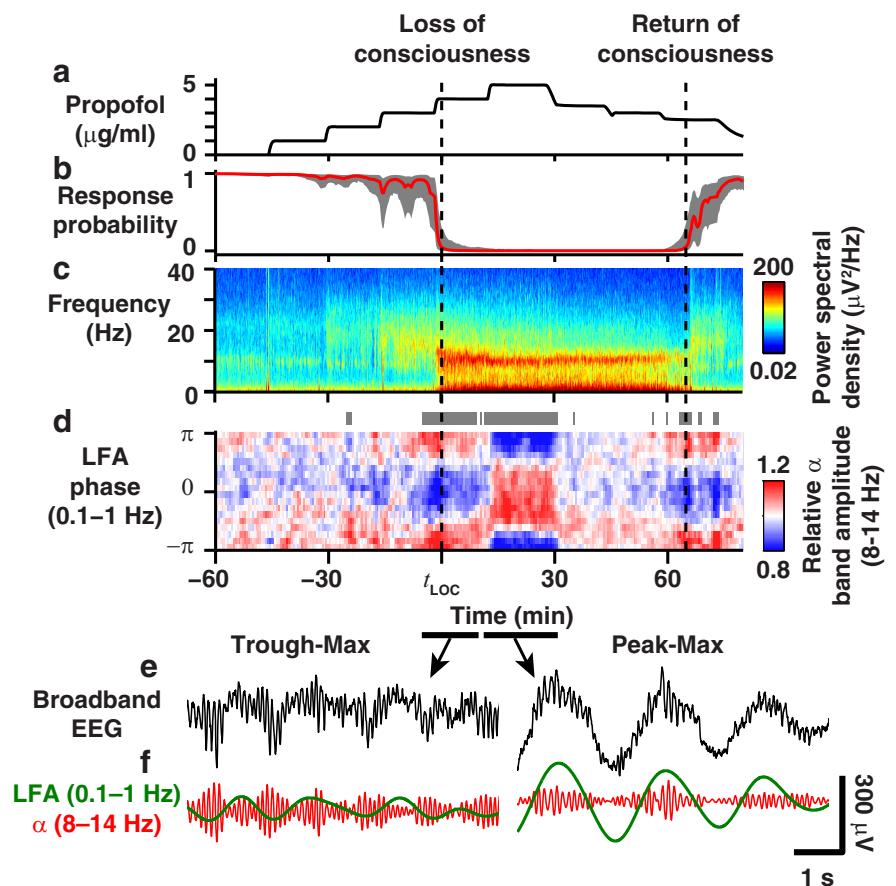


Figure 1. Phase-amplitude coupling reveals a transition during general anesthesia. *a*, Propofol effect-site concentration. *b*, Probability of response to sounds (red line indicates median; gray represents 5–95% confidence interval). *c*, Power spectrum of frontal EEG shows increased LFA and α band power during unconsciousness. *d*, Modulation of α power by LFA phase (gray bars represent $p < 0.005$, permutation test). *e, f*, Raw (*e*) and bandpass-filtered (*f*) EEG traces during trough-max (left) and peak-max (right) coupling.

density (see Fig. 1*c*) was computed using a multitaper method (window size: 2 s, 3 tapers) (Mitra and Bokil, 2008).

Phase-amplitude coupling analysis. We constructed a phase-amplitude modulogram, $M(t, \phi)$, characterizing the relative amplitude of activity in a frequency band f_{amp} as a function of the phase of the rhythm in band f_{ph} . We bandpass filtered the EEG signal, $x(t)$, to extract each frequency band of interest, $x_b(t)$, $b \in \{amp, ph\}$. Filters were chosen to adequately isolate these frequency bands while allowing temporal resolution of changes in phase-amplitude coupling, which occur within <2 min. We used symmetric finite impulse response filters designed using a least-squares approach (MATLAB function `firls`; f_{ph} passband = 0.1–1 Hz, transition bands = 0.085–0.1 and 1–1.15 Hz, attenuation in stop band ≥ 17 dB, filter order 2207; f_{amp} passband = 8–13.9 Hz, transition bands = 5.9–8.0 and 13.9–16.0 Hz, attenuation in stop band ≥ 60 dB, filter order 513). To ensure that our findings were unaffected by artifacts of filtering, we assessed statistical significance using a permutation procedure with the same filter settings (below). Next, we used a Hilbert transform to extract the instantaneous amplitude and phase.

We computed the modulogram by assigning each temporal sample to one of $N = 18$ equally spaced phase bins based on the instantaneous value of $\psi_{ph}(t)$, then averaging the corresponding values of $A_{amp}(t)$ within a 2 min epoch as follows:

$$M(t, \phi) = \frac{\int_{t-\frac{\delta t}{2}}^{t+\frac{\delta t}{2}} \int_{\phi-\frac{\delta \phi}{2}}^{\phi+\frac{\delta \phi}{2}} A_{amp}(t') \delta(\psi_{ph}(t') - \phi') d\phi' dt'}{\int_{t-\frac{\delta t}{2}}^{t+\frac{\delta t}{2}} A_{amp}(t') dt'} \quad (1)$$

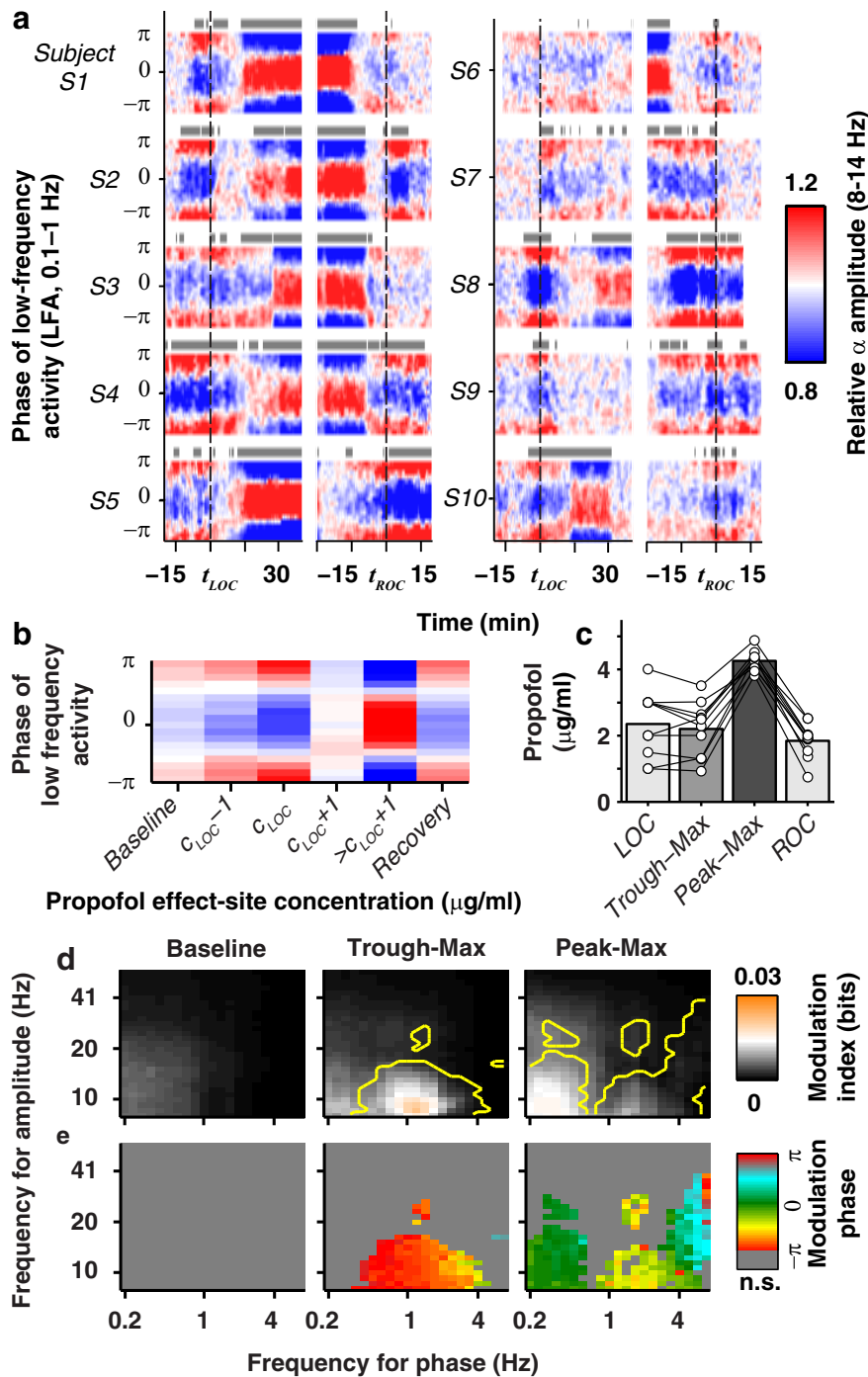


Figure 2. Stereotyped phase-amplitude coupling in unconsciousness. **a**, Frontal phase-amplitude coupling aligned to t_{LOC} and t_{ROC} (gray bars; $p < 0.005$, uncorrected). **b**, Mean coupling pattern across subjects at each drug concentration. **c**, Mean propofol concentration at LOC, ROC, and during trough-max and peak-max epochs (circles represent individual subjects). **d**, **e**, Median MI (**d**) and modulation phase (**e**) across subjects as a function of the center of the frequency bands used for phase and amplitude. Yellow contour indicates that ≥ 6 of 10 subjects showed significant modulation ($p < 0.05$; n.s., not significant).

where $\delta t = 120$ s and $\delta\phi = \frac{2\pi}{N}$. Note that $\sum_{n=1}^N M(t, \phi_n) = 1$, $\phi_n = 2\pi n/N$, so that $M(t, \phi)$ is a normalized distribution over phase bins. To reduce noise in estimated modulograms (see Figs. 1d, 2a, and 3c), we averaged the value of $M(t, \phi)$ from six frontal electrodes near Fz in the standard montage (see Fig. 4, asterisk).

The modulation index, $MI(t)$ in bits, was defined (Tort et al., 2010) as follows:

$$MI(t) = \sum_{n=1}^N M(t, \phi_n) \log_2 \frac{M(t, \phi_n)}{1/N} \tag{2}$$

We assessed statistical significance by a permutation test. We sampled 200 random time shifts, Δt , from a uniform distribution on the interval $[-60, 60]$ s. We then computed $MI_{perm}(t)$ using the original phase, $\psi_{ph}(t)$, and the shifted amplitude, $A_{amp}(t - \Delta t)$. $MI(t)$ was judged significant if it exceeded 95% of the permuted values, $MI_{perm}(t)$.

In case of significant coupling, we determined the phase of f_{ph} at which the f_{amp} amplitude is greatest by finding the phase of the sinusoid that best fit the modulogram at each time point as follows:

$$\Phi(t) \equiv \arg \left[\sum_{n=1}^N e^{i\phi_n} M(t, \phi_n) \right]$$

In recordings from individual subjects, we observed two forms of modulation: peak-max and trough-max. In the peak-max pattern, α amplitude is greatest at the surface-positive phase of the LFA; the reverse relationship occurred during trough-max coupling (see Fig. 1). We defined baseline (before propofol onset), trough-max, and peak-max epochs for each subject to analyze the spatial and frequency-dependent properties during each state (see Figs. 2c–e and 4a–c). During the unconscious period, from LOC to ROC, we tested each 2 min window for significant phase-amplitude coupling. A window was significant if the average modulation index (MI) across six frontal electrodes exceeded the average of the 95th percentile of the shuffled MI at the same set of electrodes. For each unconscious epoch with significant coupling, we defined the epoch as trough-max if $|\Phi(t) - \pi| < \frac{\pi}{4}$, and peak-max if

$$|\Phi(t)| < \frac{\pi}{4}$$

Spatial analysis. To analyze the scalp topography of phase-amplitude coupling and EEG power (see Fig. 4a,b), we generated scalp maps using subjects' individually measured electrode locations. We combined the interpolated maps across subjects by taking the median.

To estimate the spatial distribution of cortical currents responsible for peak- and trough-max EEG coupling, we performed source localization analysis of the EEG signal using the minimum norm estimate (MNE) (Hämäläinen et al., 1993) followed by phase-amplitude coupling analysis of the estimated cortical current sources. Freesurfer (Dale et al., 1999) was used to reconstruct tissue surfaces for the forward model based on high-resolution structural MRI obtained for each subject (T1 MPRAGE, 1.3 mm slice thickness, 1.3×1 mm in-plane resolution, TR/TE = 2530/3.3 ms, 7° flip angle; Siemens Trio 3 Tesla MR scanner). A three layer boundary element forward model was constructed using MNE software (Hämäläinen et al., 1993). One subject was excluded from localization analysis because the number of bad channels prevented accurate source estimation. Localization analysis used a reduced-dimension source space of 1284 patches of

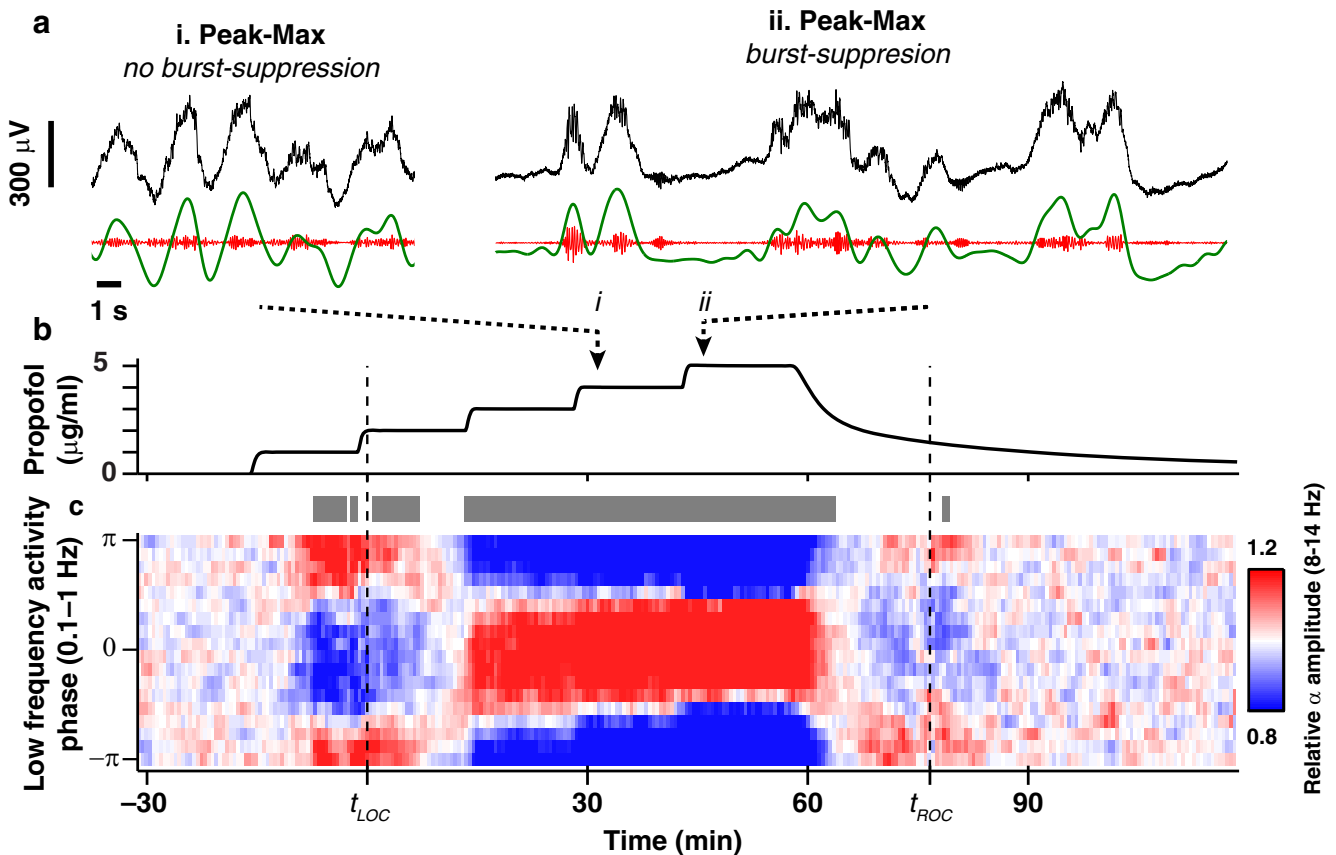


Figure 3. Peak-max coupling is not identical with burst suppression. *a*, Examples of frontal EEG records during epochs showing peak-max coupling with (*ii*) or without (*i*) burst suppression. *b*, Time course of propofol concentration. *c*, Phase-amplitude modulogram (average of 6 frontal electrodes) shows consistent peak-max coupling in both burst suppression and nonburst suppression periods.

uniform current density, each ~ 1.25 cm in diameter (Limpiti et al., 2006). Source current time series estimated by MNE were used to calculate the MI. To test significance within each patch, we resampled phase and amplitude from within each subject's trough- or peak-max epoch to construct a null distribution for the MI. These were combined across subjects using surface-based registration to an average cortical surface (Fischl et al., 1999). A p value for each patch was obtained by fitting a γ distribution to the group average null distribution; validity of the γ distribution was confirmed using Pearson's χ^2 test (0.95 confidence level). Finally, we used the p values to control the false discovery rate at $q < 0.01$ (Benjamini and Yekutieli, 2001).

Intracranial electrocorticography. Eight patients (5 male) with epilepsy intractable to medication were implanted with intracranial subdural electrocorticography (ECoG) electrodes for clinical monitoring (1 cm spacing, AdTech). Informed consent was obtained from all patients in accordance with the local institutional review board. Electrode placement was determined solely by clinical criteria, and covered regions within temporal, frontal, and parietal cortices (7 of 8 patients in the left hemisphere). Recordings were collected during surgery for electrode explantation. Anesthesia was administered as a bolus of propofol according to standard clinical protocol based on the anesthesiologist's clinical judgment. ECoG was sampled at 500 Hz with a single reference placed facing the dura in the posterior parietal region. After visual rejection of bad channels, we applied the same analysis procedures used for the EEG data (above). We used individual subjects' anatomical MRI and CT to localize electrodes with respect to the cortical surface (Dykstra et al., 2012). These locations were mapped to an average reference brain and combined across subjects for display (see Fig. 4*d*) (Dale et al., 1999).

Results

Here we report that the general anesthetic drug propofol evokes distinct unconscious brain states with opposite patterns of phase-

amplitude coupling and unique source distributions. Power spectral analysis showed that β power (12–20 Hz) increased at subanesthetic concentrations before LOC, followed by a sustained increase in LFA (0.1–1 Hz) and a frontally organized α rhythm (8–14 Hz) throughout the period of unconsciousness (Fig. 1*c*) (Gugino et al., 2001; Murphy et al., 2011; Supp et al., 2011; Purdon et al., 2013). By analyzing cross-frequency phase-amplitude coupling, we found that the frontal α rhythm during unconsciousness waxed and waned at specific phases of the LFA (Fig. 1*d*; gray bars; $p < 0.005$, permutation test). This coupling was visible in raw EEG traces (Fig. 1*e,f*).

Two distinct patterns of phase-amplitude coupling occurred during the unconscious period. At the threshold propofol concentration for LOC, t_{LOC} α amplitude was largest during the surface-negative phase of the LFA (trough-max). After an increase in propofol concentration, the phase-amplitude relationship abruptly reversed, with maximum α amplitude at the surface-positive phase of the LFA (peak-max). The transition between trough- and peak-max coupling occurred within a few minutes, after which the peak-max pattern remained until the propofol concentration was reduced. The change in phase-amplitude coupling did not coincide with the major increase in low-frequency EEG power, which occurred at LOC (Fig. 1*c*). This highlights the need for cross-frequency analysis to detect the shift in network dynamics.

All of our study subjects ($n = 10$) showed significant trough-max coupling during the transition to and/or recovery from unconsciousness, and eight showed significant peak-max coupling at the highest propofol concentrations (5 $\mu\text{g/ml}$) (Fig. 2*a–c*).

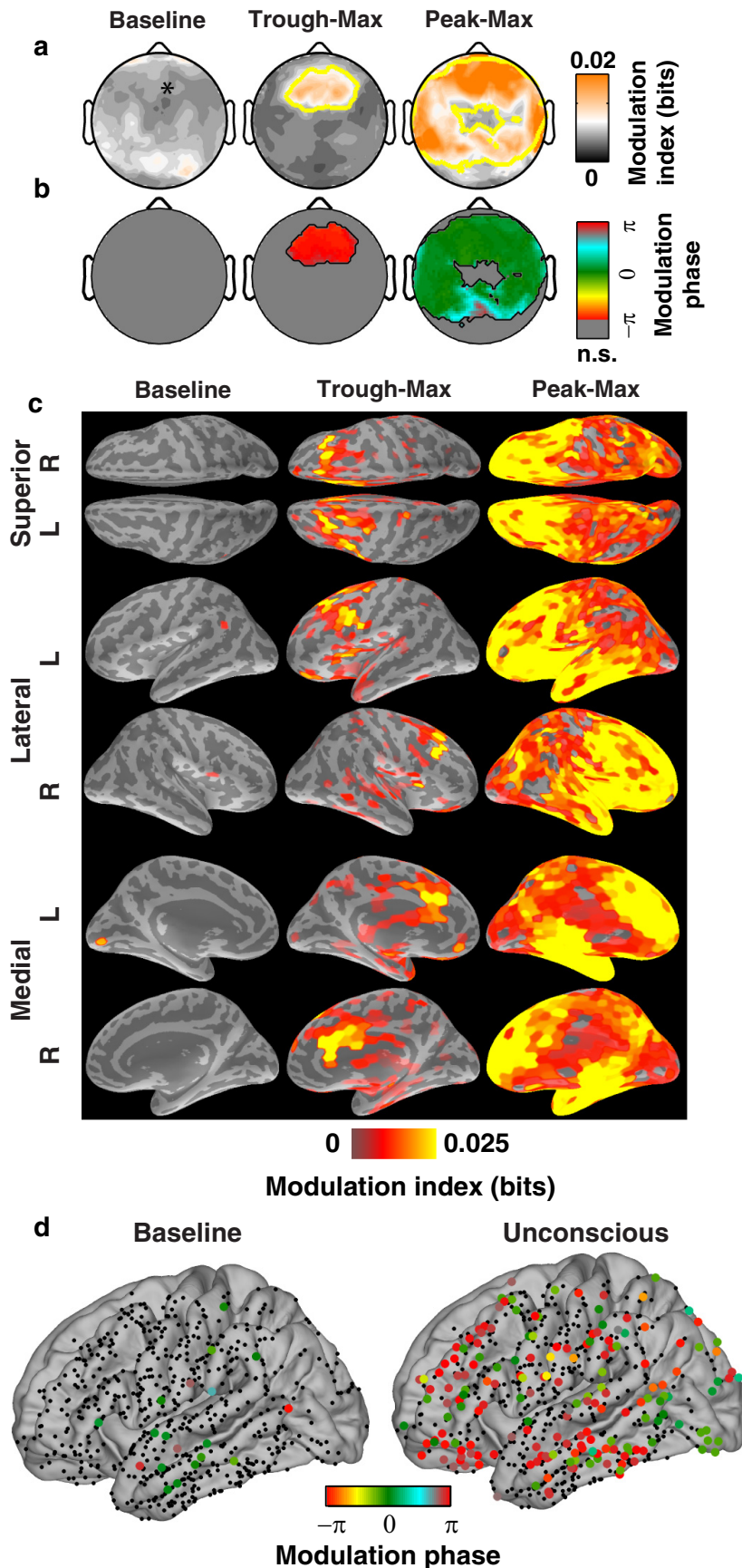


Figure 4. Spatial distribution of phase-amplitude coupling. *a, b*, Scalp distribution of MI (*a*) and phase (*b*) (median across 10 subjects). *Location of frontal electrodes used in Figs. 1, 2, and 3. *a*, Yellow contour indicates locations where at least 6 of 10

Overall, coupling was significant at frontal locations during 67% of unconscious epochs; only 11% were significant before propofol administration. The median MI, a measure of coupling strength (Materials and Methods), doubled from 6×10^{-3} bits at baseline to 12×10^{-3} bits after LOC ($p < 10^{-3}$, Mann–Whitney *U* test).

We next examined the frequency dependence of phase-amplitude coupling. Although significant phase-amplitude coupling was observed in some subjects while they were awake before LOC (Fig. 1*a*) (He et al., 2010), overall coupling before propofol administration was not consistent across subjects for any of the frequencies we tested (0.2–50 Hz; Fig. 2*d,e*). After LOC, phase-amplitude coupling was concentrated within the LFA and α bands. Trough-max coupling linked LFA and δ phase (0.4–4 Hz) with α and low β amplitude (8.3–17 Hz). During peak-max epochs, we found separate patterns of coupling between α amplitude and the LFA (0.1–1 Hz) and δ (1–4 Hz) bands. α amplitude was highest at the peaks of the LFA (Fig. 2*e*, green), whereas coupling to the δ band peaked $\sim -\pi/2$ (Fig. 2*e*, yellow).

Profound unconsciousness during general anesthesia, coma, and hypothermia can evoke a burst suppression pattern in which high-frequency activity alternates with isoelectric periods (Steriade et al., 1994; Brown et al., 2010). Burst suppression is a distinct state from sleep slow waves and slow oscillations during general anesthesia, which are more regular and alternate at a faster rate (Ching et al., 2012). In our study, 4 of 10 subjects entered a state of burst suppression at the highest propofol concentration. These subjects exhibited peak-max coupling during both burst suppression and nonburst suppression epochs (Fig. 3). Peak-max coupling is therefore not simply a consequence of burst suppression but instead represents a network state, which can occur at lower anesthetic drug doses.

Peak- and trough-max coupling had distinct spatial profiles over the scalp and across cortical regions. Traditional

subjects had significant modulation ($p < 0.05$; n.s., not significant). *c*, Average MI at cortical patches estimated by source localization analysis of the EEG. Only patches with significant modulation are included (1% false discovery rate). *d*, Locations of intracranial cortical surface electrodes ($n = 605$ sites, 8 patients), mapped to an average cortical surface. Colored points indicate modulation phase of electrodes with significant phase-amplitude coupling.

frequency-band analysis has identified the occipital-to-frontal shift in low-frequency (<40 Hz) scalp EEG power as a hallmark of general anesthesia (Gugino et al., 2001; Cimenser et al., 2011; Purdon et al., 2013). During the transition to unconsciousness, we found that trough-max coupling of α amplitude with LFA phase was likewise concentrated at frontal electrodes (Fig. 4*a,b*). However, peak-max coupling dominated activity throughout frontal, temporal, and postero-central regions. We used each subject's anatomical MRI to reconstruct cranial tissue surfaces and perform biophysical model-based source localization using a minimum norm estimation algorithm (Hämäläinen et al., 1993) (Fig. 4*c*). This procedure is biased toward distributed cortical sources, so our results represent a conservative estimate of localization. We found significant trough-max coupling in anterior cingulate and frontal cortices bilaterally, whereas peak-max coupling extended throughout much of the cortex and was strongest in frontal and temporal lobes.

To directly examine the cortical sources of phase-amplitude coupled activity with high spatial resolution, we recorded intracranial ECoG using subdural electrode grids in 8 epilepsy patients during induction of general anesthesia with propofol (605 total electrodes). After LOC, significant coupling appeared in frontal, occipital, and temporal cortices (Fig. 4*d*). The sign of the referential ECoG varies depending on the geometry of local sources, resulting in a bimodal distribution of coupling phase concentrated at 0 and π (Fig. 4*d*, green and red, respectively).

Discussion

Our data show that propofol consistently evokes two distinct cortical states with opposite phase-amplitude coupling. These EEG patterns appear in a stereotyped progression during the induction of and recovery from unconsciousness. In contrast with phase-amplitude coupling observed during waking and sleep states (He et al., 2010), the patterns we observed critically involve the frontal α rhythm, which is a hallmark of general anesthesia (Feshchenko et al., 2004; Breshears et al., 2010; Brown et al., 2010; Purdon et al., 2013). Peak-max coupling resembles the well-studied slow oscillation (Steriade et al., 1993), in which scalp-positive waves are associated with transient activated cortical UP/ON states showing increased broadband EEG, local field potential power, and multiunit activity, whereas scalp-negative waves are associated with quiescent DOWN/OFF states (Nir et al., 2011; Lewis et al., 2012). We found that peak-max coupling does not require a burst suppression activity pattern. Rather, peak-max coupling may be a general signature of unconsciousness in the cortex that precedes the onset of burst suppression.

The trough-max pattern parallels reports of increased cortical excitability and attention during the surface-negative phase of slow cortical potentials (Vanhatalo et al., 2004; He and Raichle, 2009). This pattern is localized in anterior cingulate and frontal cortices, the most rostral portion of an ascending arousal system, including brainstem, thalamic, and cortical networks that becomes more metabolically active during emergence from propofol-induced unconsciousness (Långsjö et al., 2012). Activity in anterior cingulate and frontal cortices also covaries with spontaneous fluctuations in internal awareness (Vanhaudenhuyse et al., 2011); the trough-max pattern might therefore be associated with propofol-induced changes in circuits mediating internal awareness.

The transition we have identified in cortical dynamics shows that unconsciousness during propofol general anesthesia is not a unitary brain state (Alkire et al., 2008). Instead, propofol evokes at least two distinct states with opposite patterns of cross-frequency phase-amplitude coupling that engage different cortical

networks. The fact that these opposing modulation patterns are mutually exclusive, with distinct spatial distributions, suggests that alternation between widespread cortical ON and OFF states during peak-max coupling begins only after disruption of the frontal trough-max pattern. These objective EEG landmarks enable reliable interpretation of the physiology and functional significance of cortical activity during unconsciousness.

References

- Alkire MT, Hudetz AG, Tononi G (2008) Consciousness and anesthesia. *Science* 322:876–880. [CrossRef Medline](#)
- Avidan MS, Jacobsohn E, Glick D, Burnside BA, Zhang L, Villafranca A, Karl L, Kamal S, Torres B, O'Connor M, Evers AS, Gradwohl S, Lin N, Palanca BJ, Mashour GA (2011) Prevention of intraoperative awareness in a high-risk surgical population. *N Engl J Med* 365:591–600. [CrossRef Medline](#)
- Benjamini Y, Yekutieli D (2001) The control of the false discovery rate in multiple testing under dependency. *Ann Stat* 29:1165–1188. [CrossRef](#)
- Breshears JD, Roland JL, Sharma M, Gaona CM, Freudenburg ZV, Tempelhoff R, Avidan MS, Leuthardt EC (2010) Stable and dynamic cortical electrophysiology of induction and emergence with propofol anesthesia. *Proc Natl Acad Sci U S A* 107:21170–21175. [CrossRef Medline](#)
- Brown EN, Lydic R, Schiff ND (2010) General anesthesia, sleep, and coma. *N Engl J Med* 363:2638–2650. [CrossRef Medline](#)
- Canolty RT, Edwards E, Dalal SS, Soltani M, Nagarajan SS, Kirsch HE, Berger MS, Barbaro NM, Knight RT (2006) High γ power is phase-locked to θ oscillations in human neocortex. *Science* 313:1626–1628. [CrossRef Medline](#)
- Ching S, Purdon PL, Vijayan S, Kopell NJ, Brown EN (2012) A neurophysiological-metabolic model for burst suppression. *Proc Natl Acad Sci U S A* 109:3095–3100. [CrossRef Medline](#)
- Cimenser A, Purdon PL, Pierce ET, Walsh JL, Salazar-Gomez AF, Harrell PG, Tavares-Stoeckel C, Habeeb K, Brown EN (2011) Tracking brain states under general anesthesia by using global coherence analysis. *Proc Natl Acad Sci U S A* 108:8832–8837. [CrossRef Medline](#)
- Dale AM, Fischl B, Sereno MI (1999) Cortical surface-based analysis: I. Segmentation and surface reconstruction. *Neuroimage* 9:179–194. [CrossRef Medline](#)
- Dykstra AR, Chan AM, Quinn BT, Zepeda R, Keller CJ, Cormier J, Madsen JR, Eskandar EN, Cash SS (2012) Individualized localization and cortical surface-based registration of intracranial electrodes. *Neuroimage* 59:3563–3570. [CrossRef Medline](#)
- Feshchenko VA, Veselis RA, Reinsel RA (2004) Propofol-induced alpha rhythm. *Neuropsychobiology* 50:257–266. [Medline](#)
- Fischl B, Sereno MI, Tootell RB, Dale AM (1999) High-resolution intersubject averaging and a coordinate system for the cortical surface. *Hum Brain Mapp* 8:272–284. [CrossRef Medline](#)
- Gervasoni D, Lin SC, Ribeiro S, Soares ES, Pantoja J, Nicoletis MA (2004) Global forebrain dynamics predict rat behavioral states and their transitions. *J Neurosci* 24:11137–11147. [CrossRef Medline](#)
- Gugino LD, Chabot RJ, Prichep LS, John ER, Formanek V, Aaglio LS (2001) Quantitative EEG changes associated with loss and return of consciousness in healthy adult volunteers anaesthetized with propofol or sevoflurane. *Br J Anaesth* 87:421–428. [CrossRef Medline](#)
- Hämäläinen M, Hari R, Ilmoniemi RJ, Knuutila J, Lounasmaa OV (1993) Magnetoencephalography: theory, instrumentation, and applications to noninvasive studies of the working human brain. *Rev Mod Phys* 65:413–497. [CrossRef](#)
- He BJ, Raichle ME (2009) The fMRI signal, slow cortical potential and consciousness. *Trends Cogn Sci* 13:302–309. [CrossRef Medline](#)
- He BJ, Zempel JM, Snyder AZ, Raichle ME (2010) The temporal structures and functional significance of scale-free brain activity. *Neuron* 66:353–369. [CrossRef Medline](#)
- Jensen O, Colgin LL (2007) Cross-frequency coupling between neuronal oscillations. *Trends Cogn Sci* 11:267–269. [CrossRef Medline](#)
- Lakatos P, Karmos G, Mehta AD, Ulbert I, Schroeder CE (2008) Entrainment of neuronal oscillations as a mechanism of attentional selection. *Science* 320:110–113. [CrossRef Medline](#)
- Långsjö JW, Alkire MT, Kaskinoro K, Hayama H, Maksimow A, Kaisti KK, Aalto S, Aantaa R, Jääskeläinen SK, Revonsuo A, Scheinin H (2012) Re-

- turning from oblivion: imaging the neural core of consciousness. *J Neurosci* 32:4935–4943. [CrossRef Medline](#)
- Lewis LD, Weiner VS, Mukamel EA, Donoghue JA, Eskandar EN, Madsen JR, Anderson WS, Hochberg LR, Cash SS, Brown EN, Purdon PL (2012) Rapid fragmentation of neuronal networks at the onset of propofol-induced unconsciousness. *Proc Natl Acad Sci U S A* 109:E3377–E3386. [CrossRef Medline](#)
- Limpiti T, Van Veen BD, Wakai RT (2006) Cortical patch basis model for spatially extended neural activity. *IEEE Trans Biomed Eng* 53:1740–1754. [CrossRef Medline](#)
- Mitra P, Bokil H (2008) Observed brain dynamics. Oxford: Oxford UP.
- Molae-Ardekani B, Senhadji L, Shamsollahi MB, Wodey E, Vosoughi-Vahdat B (2007) Delta waves differently modulate high frequency components of EEG oscillations in various unconsciousness levels. *Conf Proc IEEE Eng Med Biol Soc* 2007:1294–1297. [Medline](#)
- Mukamel EA, Wong KF, Prerau MJ, Brown EN, Purdon PL (2011) Phase-based measures of cross-frequency coupling in brain electrical dynamics under general anesthesia. *Conf Proc IEEE Eng Med Biol Soc* 2011:1981–1984. [CrossRef Medline](#)
- Murphy M, Bruno MA, Riedner BA, Boveroux P, Noirhomme Q, Landsness EC, Bricchant JF, Phillips C, Massimini M, Laureys S, Tononi G, Boly M (2011) Propofol anesthesia and sleep: a high-density EEG study. *Sleep* 34:283–291. [Medline](#)
- Nir Y, Staba RJ, Andrillon T, Vyazovskiy VV, Cirelli C, Fried I, Tononi G (2011) Regional slow waves and spindles in human sleep. *Neuron* 70:153–169. [CrossRef Medline](#)
- Nunez PL, Pilgreen KL (1991) The spline-Laplacian in clinical neurophysiology: a method to improve EEG spatial resolution. *J Clin Neurophysiol* 8:397–413. [CrossRef Medline](#)
- Purdon PL, Pierce ET, Mukamel EA, Prerau MJ, Walsh JL, Wong KF, Salazar-Gomez AF, Harrell PG, Sampson AL, Cimenser A, Ching S, Kopell NJ, Tavares-Stoeckel C, Habeeb K, Merhar R, Brown EN (2013) Electroencephalogram signatures of loss and recovery of consciousness from propofol. *Proc Natl Acad Sci U S A* 110:E1142–E1151. [CrossRef Medline](#)
- Roopun AK, Kramer MA, Carracedo LM, Kaiser M, Davies CH, Traub RD, Kopell NJ, Whittington MA (2008) Temporal interactions between cortical rhythms. *Front Neurosci* 2:145–154. [CrossRef Medline](#)
- Smith AC, Shah SA, Hudson AE, Purpura KP, Victor JD, Brown EN, Schiff ND (2009) A Bayesian statistical analysis of behavioral facilitation associated with deep brain stimulation. *J Neurosci Methods* 183:267–276. [CrossRef Medline](#)
- Steriade M, Nuñez A, Amzica F (1993) A novel slow (< 1 Hz) oscillation of neocortical neurons in vivo: depolarizing and hyperpolarizing components. *J Neurosci* 13:3252–3265. [Medline](#)
- Steriade M, Amzica F, Contreras D (1994) Cortical and thalamic cellular correlates of electroencephalographic burst suppression. *Electroencephalogr Clin Neurophysiol* 90:1–16. [CrossRef Medline](#)
- Supp GG, Siegel M, Hipp JF, Engel AK (2011) Cortical hypersynchrony predicts breakdown of sensory processing during loss of consciousness. *Curr Biol* 21:1988–1993. [CrossRef Medline](#)
- Tort AB, Komorowski R, Eichenbaum H, Kopell N (2010) Measuring phase-amplitude coupling between neuronal oscillations of different frequencies. *J Neurophysiol* 104:1195–1210. [CrossRef Medline](#)
- Vanhatalo S, Palva J, Holmes M, Miller J, Voipio J, Kaila K (2004) Infraslow oscillations modulate excitability and interictal epileptic activity in the human cortex during sleep. *Proc Natl Acad Sci U S A* 101:5053–5057. [CrossRef Medline](#)
- Vanhau den huuse A, Demertzi A, Schabus M, Noirhomme Q, Bredart S, Boly M, Phillips C, Soddu A, Luxen A, Moonen G, Laureys S (2011) Two distinct neuronal networks mediate the awareness of environment and of self. *J Cogn Neurosci* 23:570–578. [CrossRef Medline](#)